*Journal of Structural Geology*, Vol. 13, No. 6, pp. 657 to 666, 1991
Printed in Great Britain

0191-8141/91 $03.00+0.00


# Prism ⟨*c*⟩ slip in the quartzites of the Oakhurst Mylonite Belt, California

JOHN M. GARBUTT and CHRISTIAN TEYSSIER

Department of Geology and Geophysics, University of Minnesota, Minneapolis, MN 55455, U.S.A.

(*Received* 5 *July* 1989; *accepted in revised form* 10 *December* 1990)

**Abstract**—Quartz *c*-axis fabrics from 21 amphibolite facies quartzites of the Oakhurst Mylonite Belt, California, suggest that prism ⟨*c*⟩, prism ⟨*a*⟩ and basal ⟨*a*⟩ slip systems were activated during deformation. Qualitative two-dimensional kinematic models, consistent with meso- and microscopic shear criteria, are constructed based on a regime of combined pure and simple shear. In this kinematic framework, most of the observed *c*-axis fabric patterns of the Oakhurst Mylonite Belt can be explained if prism ⟨*c*⟩ slip was dominant during the early increments of deformation, until a transition to dominant basal ⟨*a*⟩ slip occurred. An apparent relationship between grain size and type of crystallographic fabric is interpreted as resulting from some quartz (syntectonic vein quartz) having recorded only the latest increments of deformation.

Comparison with the metamorphic evolution of fault zones of similar tectonic origin in California suggests that prism ⟨*c*⟩ slip was enhanced by the circulation of hot fluids which hydrolytically weakened quartz and allowed prism ⟨*c*⟩ slip to occur at relatively low temperature.

## INTRODUCTION

PLASTICALLY deformed quartzites show distinctly different types of crystallographic preferred orientation (CPO, used throughout the text in reference to the *c*-axis preferred orientation), governed by (1) the magnitude of finite strain, (2) the type of strain history, (3) the particular combination of slip systems active during deformation and (4) the role of dynamic recrystallization (Lister *et al.* 1978, Lister & Paterson 1979, Lister & Hobbs 1980, Hobbs 1985, Jessell 1988a).

The magnitude of strain not only has an effect on the orientation of CPO maxima, but it also has an intrinsic role in determining the intensity of those maxima (Lister & Hobbs 1980, Jessell 1988b). If the strain history is non-coaxial, i.e. involving simple shear, then the resulting CPO will exhibit a monoclinic or trigonal symmetry (although after infinite shear an orthorhombic symmetry will develop), whereas if the strain history is coaxial, i.e. pure shear, then the resulting CPO will always show orthorhombic symmetry. This relationship has been used to gain kinematic information about deformation events (see Bouchez *et al.* 1983, for a review).

Experimental studies on the deformation of quartz show that intracrystalline slip occurs at low to moderate temperatures if there is a trace of water present in the crystal lattice (Avé Lallemant & Carter 1971, Hobbs *et al.* 1972, Tullis & Tullis 1972, Blacic 1975). It is found that basal slip and rhomb slip are the easiest, but that at high temperature, two common prismatic slip systems occur, prism ⟨*a*⟩ {1010}⟨1210⟩, and prism ⟨*c*⟩ {1010}[0001] (Nicolas & Poirier 1976, p. 201).

Temperature is not the only intrinsic parameter determining slip system (Hobbs 1985). It has been shown in the laboratory that the presence of water may cause a 20-fold weakening (Griggs & Blacic 1965) and that fluids have an important effect on operative slip systems in natural quartzite (Lister & Dornsiepen 1982, Bouchez *et al.* 1984, Blumenfeld *et al.* 1986). Water has been shown to have circulated in areas where possible prism ⟨*c*⟩ slip has occurred (Behr 1980, Blumenfeld *et al.* 1986, Duebendorfer & Houston 1987), and indeed prism ⟨*c*⟩ slip has been demonstrated in experiments on the deformation of synthetic crystals with a high water content (Blacic 1975, Linker & Kirby 1981). In addition, water tends to diffuse preferentially along the *c* direction in quartz (Linker & Kirby 1981). Blacic (1975) concludes that this anisotropy could lead to the enhancement of prism ⟨*c*⟩ slip over basal ⟨*a*⟩ in hydrolytically weakened quartz. However, Gilletti & Yund (1984) contest this point on the basis of oxygen diffusion coefficient data.

### *Evidence for prism* ⟨c⟩ *slip in nature, and alternative models*

In naturally deformed quartzites, it is found that in almost all the specimens for which CPO has been measured, the fabrics may be attributed to slip on basal ⟨*a*⟩, rhomb ⟨*a*⟩, and/or prism ⟨*a*⟩ slip systems (Lister & Williams 1979, Bouchez & Pecher 1981, Hobbs 1985, Price 1985, Law 1986, Law *et al.* 1986, Vissers 1989, to name but a few). In only five previous studies known to the authors has the CPO pattern been suggestive of prism ⟨*c*⟩ slip. These were from the Saxony granulite (Behr 1980, Lister & Dornsiepen 1982), from Galicia, Spain (Bouchez *et al.* 1984), from the Cheyenne Belt, Wyoming (Duebendorfer & Houston 1987, 1990), from the Vosges massif, France (Blumenfeld *et al.* 1986), and from the Hermitage granite in the French Massif Central (Gapais & Barbarin 1986).

In the Saxony granulite, the *c*-axis fabric patterns are associated with the concurrent operation of prism ⟨*c*⟩ and basal ⟨*a*⟩ slip systems, producing a 90° cross girdle, followed by a transition to basal ⟨*a*⟩ alone. Schmid *et al.* (1981) show a CPO pattern from the same rocks showing a single *c*-axis maximum on lineation. In the case of

the Galicia quartzite, the prism ⟨c⟩ fabric in upper amphibolite grade quartzites was argued to be post-tectonic, because of transposition of the tectonic lineation by quartz grain growth preferentially in the *c* direction. Therefore, the original CPO pattern is reminiscent of a more common prism ⟨a⟩ pattern. In the case of the Cheyenne Belt, the fabrics show a form similar to those from the Saxony granulite with one exception in which the fabric is similar to those that will be shown to occur in the Oakhurst Mylonite Belt. In the Vosges massif, workers came to the conclusion that prism ⟨c⟩ and prism ⟨a⟩ slip had occurred in a subsolidus granite deformed at or about 700–800°C. In the Hermitage granite, it was proposed that the *c*-axis maximum in a direction subparallel to the principal extension direction is the result of preferred grain growth associated with dynamic migration-recrystallization, and not intracrystalline slip, during the high-temperature deformation of a cooling, syntectonic pluton.

Where documented, it is clear that prism ⟨c⟩ slip is commonly associated with high-temperature deformation. By contrast, we describe moderate-temperature mylonitic quartzites from the Oakhurst Mylonite Belt, which also display prism ⟨c⟩ dominated fabrics. We discuss a simple kinematic model which could produce the observed crystallographic patterns, based on progressive changes in slip systems, perhaps partly controlled by progressive changes in fluid activity. This kinematic model is somewhat constrained by the independent meso- and microscopic shear criteria analyzed in these rocks.

## REGIONAL GEOLOGICAL SETTING

The Oakhurst Mylonite Belt, an arcuate body of metasediments and metavolcanics, lies in the Western Metamorphic Belt, California, and is surrounded on all sides by tonalitic plutons of the Sierra Nevada Batholith (Fig. 1). The deformation observed in the Oakhurst Mylonite Belt has previously been associated with the emplacement of the Ward Mountain leucotonalite (Bateman *et al.* 1983). Recent studies however (Garbutt 1989), have suggested that the mylonitic fabric in the Oakhurst Mylonite Belt developed during the waning stages of the Late Jurassic to Cretaceous deformation, prior to granite emplacement, in a ductile shear zone which had an oblique, east-side-down, dextral strike-slip sense of motion. This shear zone is thought to have formed as a kinematic conjugate to the Bear Mountains fault zone and Melones fault zone, both of which have similar orientations, but an opposite sense of motion (Paterson *et al.* 1987, Geffel *et al.* 1989). This is consistent with studies which show that the Western Metamorphic Belt deformed largely by pure shear, but that deformation was localized into shear zones where an increasing component of simple shear is observed (Paterson *et al.* 1989, Tobisch *et al.* 1989). This ductile deformation post-dated deformation due to the main stage of the Nevadan orogeny, which in the Western

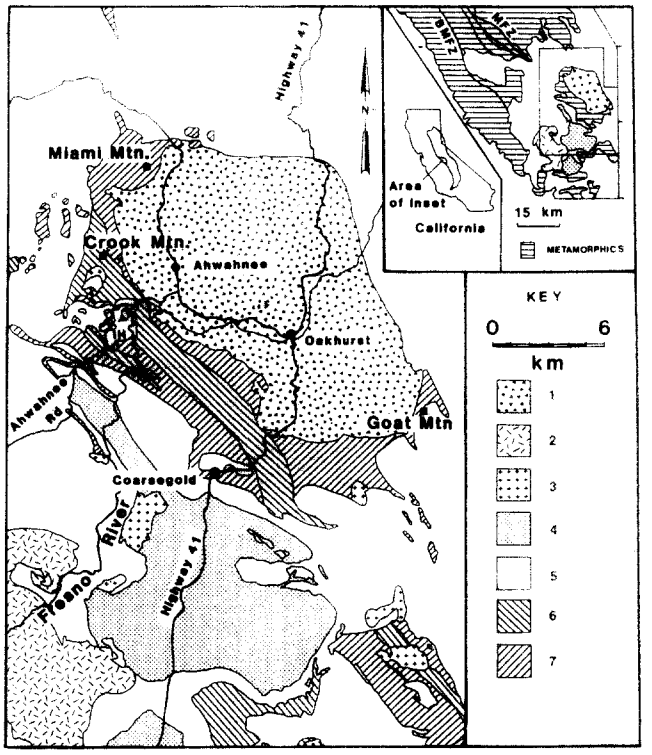


Fig. 1. Geological map of the Oakhurst Mylonite Belt, California (1 = Oakhurst Tonalite; 2 = Granodiorite of Knowles; 3 = Gabbro; 4 = Ward Mountain Leucotonalite; 5 = Blue Canyon Tonalite; 6 = Metavolcanics; 7 = Metasediments; IH = Indian Hill; BMFZ = Bear Mountain fault zone; MFZ = Melones fault zone).

Metamorphic Belt is expressed in cleavages, schistosities and folds developed under greenschist facies conditions.

The Oakhurst Mylonite Belt is found to be in the epidote–amphibolite facies of regional metamorphism (600°C maximum temperature), although its edges have recorded a contact metamorphism up to staurolite + cordierite ± garnet ± sillimanite grade, which clearly overprints the former (Garbutt 1989). This metamorphic history, along with the fabric of the Oakhurst Mylonite Belt, bears similarities to that of the Bear Mountains fault zone, the metamorphism of which is associated with the influx of heated fluids (Tobisch *et al.* 1989). Fluid influx is also invoked as the cause of the syn-kinematic amphibolite facies metamorphism of the Oakhurst Mylonite Belt (Garbutt 1989). This correlation adds weight to the argument that fluids played an important role in the development of prism ⟨c⟩ slip in the rocks described in this paper.

The metasediments of the Oakhurst Mylonite Belt are divided into two banded domains, one to the west and one to the east of a central belt of metavolcanics (Fig. 1). All of these rocks contain a pervasive mylonitic fabric, with foliation defined by grainsize and compositional banding, and lineation defined by flattened rod-shaped polycrystalline quartz ribbons, minor crenulations of foliation, and alignment of long biotite grains. The strike of the mylonitic foliation faithfully follows the arcuate shape of the Oakhurst Mylonite Belt, and the foliation planes dip so as to form an upwardly diverging fan. Lineation is in general steeply plunging, with a pitch to

the south, indicating a component of strike-slip motion (Garbutt 1989). The metasediments contain rare isoclinal folds, whose axial planes are parallel to the mylonitic foliation, and whose hinges are subparallel to the lineation. For the purpose of this paper, it is assumed that the foliation and lineation in these mylonites developed in a near plane strain regime, such that the kinematic history can be reduced to the relative proportion of simple and pure shear.

Kinematic indicators within the metasediments occur on two scales. On the hand sample scale discrete shear zones from which a sense of shear may be derived, cut across the foliation. On a microscopic scale, mica and hornblende fish may be used to derive a sense of shear. These are not of the classical form as described in the literature (Simpson & Schmid 1983, Lister & Snoke 1984, Simpson 1986), but at a smaller angle to foliation, with a greater aspect ratio and a more recrystallized appearance. A study of these indicators (Garbutt 1989) has shown that the Oakhurst Mylonite Belt records a predominantly east-side-down sense of motion in the metasediments. In the metavolcanics however, both mica and hornblende fish show an equal distribution of east- and west-side-down indicators on all scales. It is suggested that, due to rheological differences, simple shear played a more important role in the quartz-rich metasediments than the metavolcanics which seem to have recorded dominant pure shear.

## MICROSTRUCTURAL RELATIONS IN METASEDIMENTS

The microstructural relations within the Oakhurst Mylonite Belt quartzose metasediments are summarized in Table 1. In general, the metasediments are composed of alternating mica-rich (up to 15%) and mica-poor layers several millimeters thick, and the recrystallized grainsize of quartz is inversely proportional to mica content (see Table 1). The more coarsely recrystallized layers are interpreted to be relict quartz veins developed prior to or during mylonitic deformation. Quartz grains are polygonized irrespective of grain size, and are rarely elongated. Deformation bands and lamellae are commonly observed in orientations both parallel and perpendicular to the trace of *c*-axes; and in a few cases, the deformation bands normal to the *c*-axis trace seem to be kinked by a later set parallel to *c*-axis. Sense of shear derived from mica fish demonstrates a consistent, well developed east-side-down pattern (Table 1).

Table 1. Microstructural characteristics of the Oakhurst Mylonite Belt quartzites, for which the *c*-axis fabric was measured. The microfabric types (Groups A–E) refer to the different groups defined in Fig. 2

| Sample # | Quartz grain size (mm) | Mica content (%) | Microstructural characteristics g.b.: grain boundaries | d.b.: deformation bands | Shear sense from mica fish | Microfabric (Fig. 2) |
|---|---|---|---|---|---|---|
| 19 | 0.25 | 10 | Polygonized g.b. | | East-side-down | Group D(i) |
| | 1.1 | 1 | Straight, serrated g.b. | d.b. ⊥ and // to c trace | | Group A |
| 21 | 0.5 | 2 | Straight/polygonized and serrated g.b. | d.b. ⊥ and // to c trace | East-side-down | Group C(i) |
| | 2.0 | 2 | Curved/serrated g.b. | | | Group A |
| 22 | 0.1 | 15 | Curved/polygonized g.b. No d.b. | d.b. ⊥ and // to c trace | 80% east-side- and 20% west-side-down | Group D(ii) |
| | 0.25 | 1 | Curved/polygonized and serrated g.b. | | | Group C(ii) |
| | 1.0 | 1 | Curved/serrated g.b. | | | Group B(i) |
| 25B | 0.1 | 11 | Polygonized g.b. No. d.b. | | East-side-down | Group D(ii) |
| | 0.25 | 2 | Curved/serrated g.b. | d.b. ⊥ to a trace | | Group C(ii) |
| 37B | 0.25 | 15 | Straight and curved/serrated g.b. | d.b. ⊥ and // to c trace | 70% east-side- and 30% west-side-down | Group D(ii) |
| | 2.0 | 1 | Straight and curved/serrated g.b. | | | Group A |
| 42B | 0.25 | 8 (hbl. + mica) | Polygonized texture. No d.b. | | East-side-down + hornblende fish | Group D(i) |
| 45 | 0.25 | 10 | Polygonized. No. d.b. | | East-side-down | Group C(ii) |
| | 0.5 | 1 | Straight and serrated g.b. | d.b. ⊥ and // to c trace | | |
| 47A | 0.1 | 12 | Polygonized. No d.b. | | East-side-down | Group D(i) |
| | 0.75 | 1 | Curved and serrated g.b. | d.b. ⊥ and // to c trace | | Group B(ii) |
| 65 | 0.1 | 10 | Polygonized. No visible d.b. | | 60% east-side- and 40% west-side-down | Group D(i) |
| 96 | 0.1 | 12 | Polygonized. No visible d.b. | | Non-determinable | Group D(i) |
| 97A | 0.05 | 8 | Polygonized. No visible d.b. | | 70% east-side- and 30% west-side-down | Group E |
| 114 | 0.5 | 2 | Polygonized. No visible d.b. | | East-side-down | Group C(ii) |
| 116 | 0.05 | 17 | Polygonized. No visible d.b. | | Non-determinable | Group D(i) |

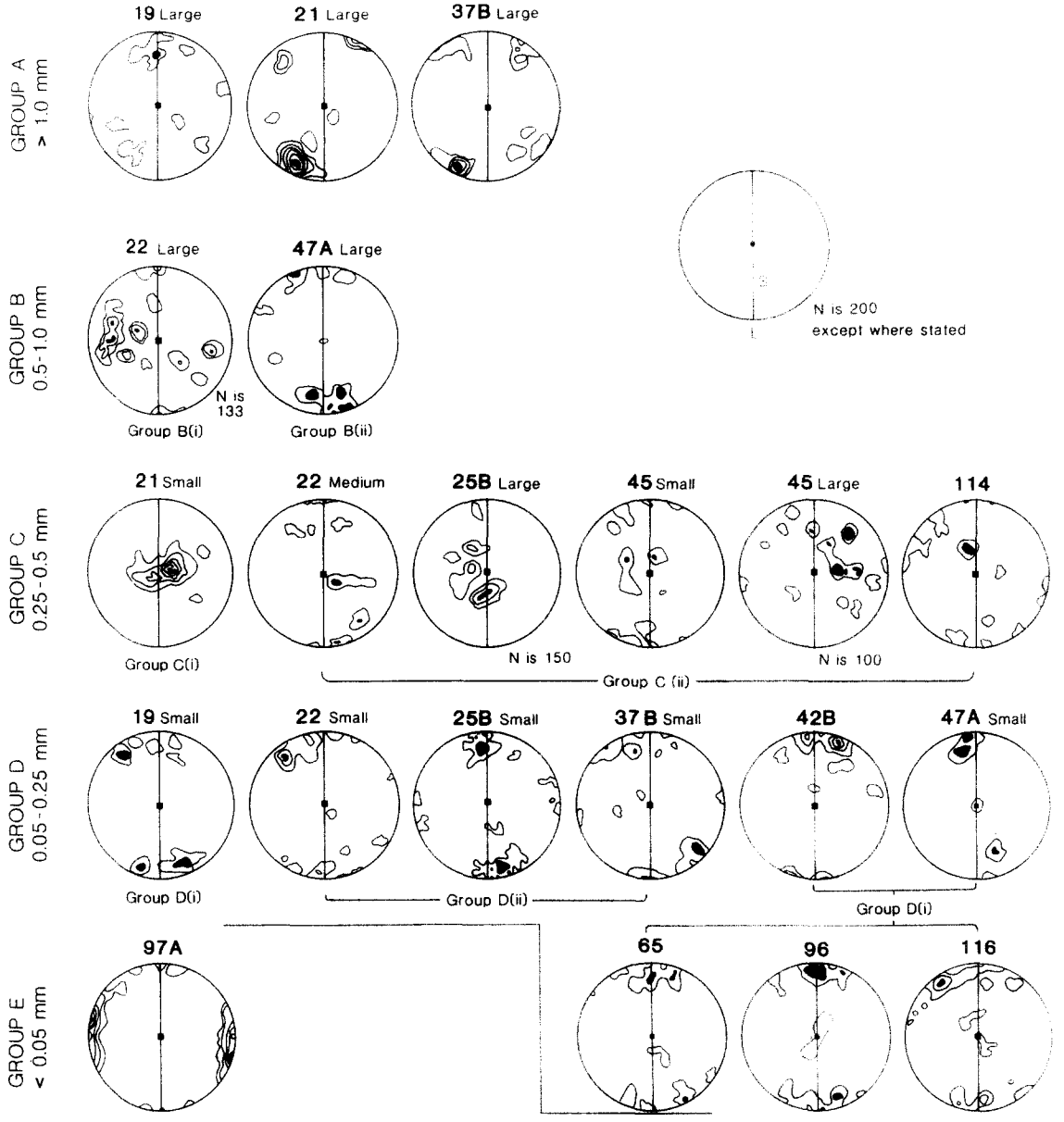


Fig. 2. Quartz *c*-axis fabric diagrams represented as a function of grainsize. Schmidt equal-area projections are contoured at 2, 4, 6, 8, 10 and 12%; (S = foliation; L = lineation).

## MEASURED QUARTZ *c*-AXIS FABRICS

In all cases, the ribbons of differing grainsizes within a single thin section were measured separately, and consequently the resulting orientation diagrams are presented with respect to the average grainsize in the ribbons measured (Fig. 2). Group A–C quartzites are made up of polycrystalline quartz layers which contain relatively little mica, and are thought to have been mostly vein quartz.

Since lineation is steeply plunging in the field (from 60° to 90°), the diagrams in Fig. 2 conveniently represent a near cross-sectional view containing lineation and perpendicular to foliation, and in a sense such that the inner part of the Oakhurst Mylonite Belt arc is on the right-hand side of each plot (i.e. viewer looking north). The sample localities are shown in Fig. 3, which also displays the sense of shear derived from mica fish in each sample. Five different grainsize groups, each of which is characterized by a differing *c*-axis fabric, can be delineated (Fig. 2).

Group A *c*-axis fabrics all come from quartz ribbons with an average grainsize greater than 1 mm in the smallest dimension of the grain. Where the fabric is well developed, a main maximum at 25–30° clockwise from lineation and a subsidiary maximum at 90° to this are exhibited. Group B *c*-axis fabrics (average grainsize between 0.5 and 1.0 mm) are less consistent. They show one maximum in the projection plane, but rotated 5–15° anticlockwise from lineation. In one sample (22 Large) a girdle 5° off perpendicular to lineation, in a clockwise direction (Group Bi) is present. Thus, the angle in the projection plane between the pole to the girdle and the former maximum is approximately 15°. Group C fabrics are observed in the grainsize range 0.25–0.5 mm. All of these fabrics show a well developed maximum, approximately perpendicular to lineation and in the plane of foliation (Group Ci). In the majority of cases, there is

also a weak maximum in a position rotated 5–20° anticlockwise from lineation in the projection plane (Group Cii).

Group D fabrics occurring in the grainsize 0.05–0.25 mm, are well defined and very consistent. They all contain a maximum of *c*-axes at or around the lineation. The majority of these maxima are rotated in an anticlockwise sense from lineation by up to 30°. Most of these fabrics have subsidiary maxima, or hints thereof, in positions perpendicular to lineation, either in the plane of foliation or perpendicular to foliation (Group Di). In the fabrics where both maxima occur (Group Dii), the latter tends to be slightly rotated anticlockwise from the pole to foliation.

Group E consists of only one fabric pattern measured in bands with a grainsize less than 0.55 mm. It shows a well developed maximum approximately perpendicular to foliation but slightly rotated clockwise from it, and a small subsidiary maximum on lineation.

Most of the fabrics described above are somewhat unusual and, as a result, no simple model is available to explain them. It is therefore proposed to formulate models for the production of these fabrics, by considering the effect attributed to recrystallization, the likely kinematic framework, and the operative slip systems.

## MODELS

Two groups of models can be put forward: (1) those emphasizing grain growth as an important mechanism in the development of fabrics; and (2) those attempting to

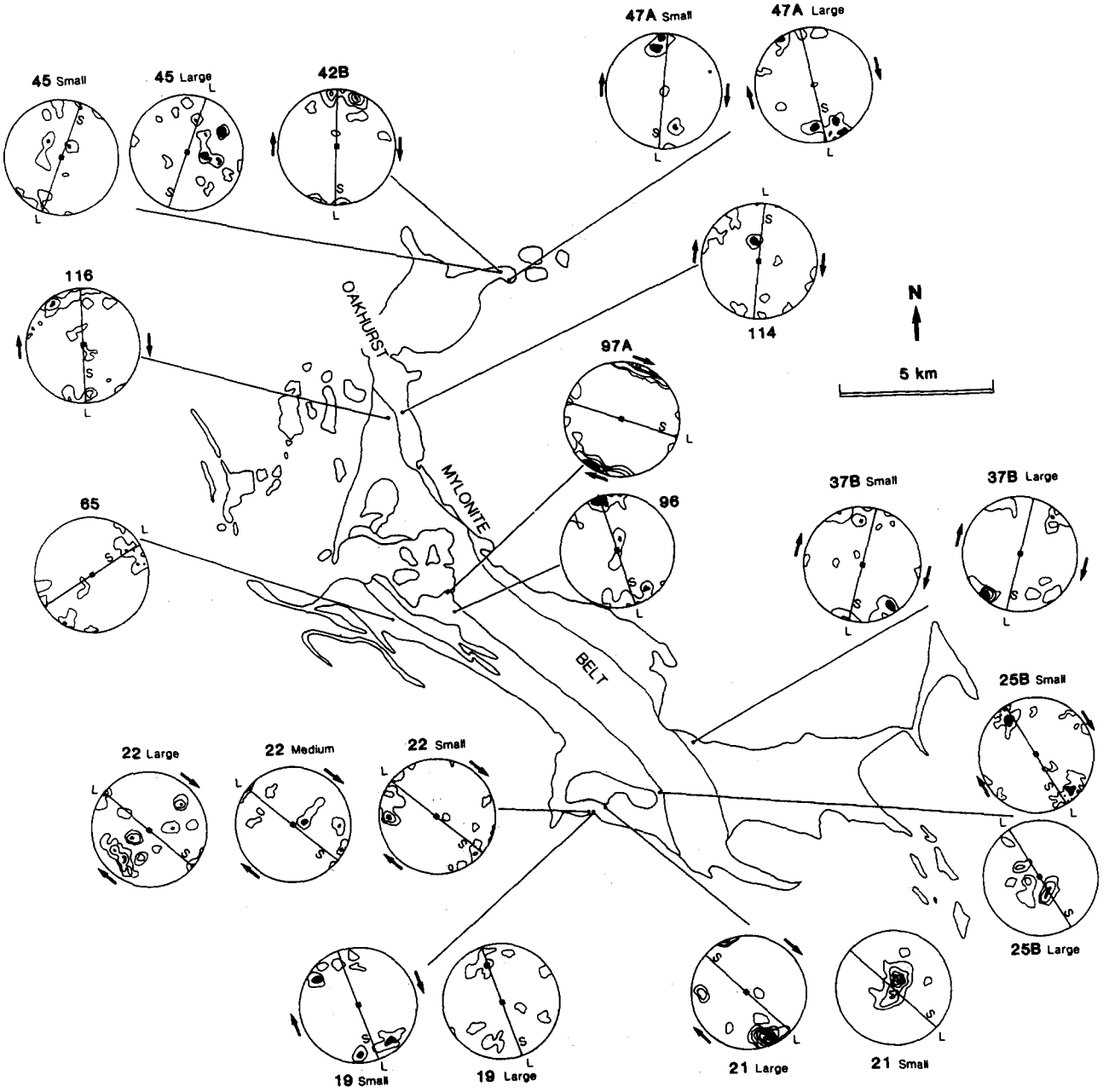


Fig. 3. Location map of samples in which quartz *c*-axis fabrics from quartzites of the Oakhurst Mylonite Belt were measured. All fabrics are oriented so that foliation dips as it does in the field, looking north (S = foliation; L = lineation). Arrows represent shear couple deduced from mica fish asymmetry; note the predominance of an east-side-down sense of shear.

explain the fabrics in terms of combinations of slip systems assuming the lineation and foliation are kinematically associated with the strain induced CPOs.

*Effect of grain growth*

In a quartzite from Galacia, Spain, Bouchez *et al.* (1984) noted a *c*-axis pattern very similar to Groups B(ii) and D(i) (Fig. 2). On the basis of the statistical orientation of rutile needles in quartz grains (the needles being elongated at right-angles to the lineation orientation defined by the quartz grains), the authors concluded that prism ⟨*c*⟩ slip was not operative. Instead, they proposed a model whereby the quartzite was originally deformed under a regime of prism ⟨*a*⟩ slip, associated with a tectonic lineation perpendicular to the present quartz lineation. Then, during a post-kinematic event, the quartz grains recrystallized, growing preferentially in the ⟨*c*⟩ direction to produce the present, proposed secondary, lineation. Thus, the CPO patterns observed are purely phantom with respect to foliation and lineation; so viewed, the *c*-axis fabrics would be in the form of classical prism ⟨*a*⟩ fabrics.

In the Oakhurst Mylonite Belt quartzites, the foliation is defined by bands of coarse and fine equant quartz grains, and the lineation by the strong stretching of biotite as well as quartz grains. In addition, the regionally subparallel lineation in the adjacent metavolcanics is defined by the strong elongation of hornblende grains. It is unlikely that all of these minerals grew in this consistent orientation without affecting the crystallographic orientation of quartz. The lineation switch model by static growth cannot apply to the Oakhurst Mylonite Belt quartzites as they clearly contain a regionally consistent stretching lineation.

Alternatively, the point maximum close to the lineation could be due to the selective dynamic (syn-kinematic) growth of grains with *c*-axes close to the maximum extension direction, as proposed by Gapais & Barbarin (1986). Grain boundary migration is powerful in producing strong maxima (Jessel 1988b) and the observation that, in the Oakhurst Mylonite Belt quartzites, prism ⟨*c*⟩ type maxima are developed in the coarsest aggregates (Groups A and B, Fig. 2) supports this hypothesis (although the finer grained Group D also shows these maxima). We are convinced that selective grain growth is a very important process in producing the observed fabrics (Culshaw & Fyson 1983), but more microstructural and microchemical work needs to be done before it is fully understood. In the next section, we assume that intracrystalline slip is the chief parameter controlling the CPO, and address kinematic models for the development of these fabrics.

*Combinations of slip systems under simple and pure shear*

As a basis for our models, we propose that the CPO is kinematically associated with the development of the foliation and lineation observed in the Oakhurst Mylonite Belt. This association is not one of rolling (Cloos 1946, Bell 1978, Lister & Price 1978) in which the steep lineation would be normal to transport in a strike-slip regime, but one of shearing in a direction subparallel to lineation, with an east-side-down sense of motion. Both mesoscopic and microscopic data support this interpretation.

The operative slip systems can be partly constrained by the position of *c*-axes in the diagrams relative to the foliation and lineation. It is assumed that intracrystalline slip is the dominant deformation mechanism, and that the meso- and microfabrics are genetically associated. If this is correct, the maxima at or around the orientation of lineation suggest prism ⟨*c*⟩ slip (Schmid *et al.* 1981, Lister & Dornsiepen 1982, Bouchez *et al.* 1984), and the other well-developed maxima suggest that both prism ⟨*a*⟩ and basal ⟨*a*⟩ slip systems were also operative during the deformation of the Oakhurst Mylonite Belt quartzites. It is emphasized that these qualitative models only deal with the geometrical aspects associated with crystal slip, and do not take into account other important phenomena such as recrystallization.

For simple strain histories such as simple shear, the CPO can be somewhat predicted for different dominant slip systems (Schmid & Casey 1986, Etchecopar & Vasseur 1987, Jessell 1988a). During progressive simple shear, the shear plane involved in the deformation stays fixed in an external reference frame, and foliation and lineation (here equated to the finite strain principal axes) rotate from an initial angle of 45° to the shear plane into parallelism with it at infinite shear (Bouchez *et al.* 1983). Thus, if shear is dominantly accommodated by basal ⟨*a*⟩ slip within grains, for a right-lateral shear sense, the *c*-axes would initially concentrate at 45° anticlockwise from lineation in the plane perpendicular to foliation and containing lineation, and would progressively rotate to a position normal to the foliation and lineation at infinite shear.

If the same shear were to be accommodated on the prism ⟨*c*⟩ slip system, then *c*-axes would first concentrate at 45° clockwise from lineation, and with progressive shear the foliation would rotate towards this maximum until it concurred with the lineation direction at infinite shear.

During progressive non-spinning pure shear (Lister & Williams 1983), the foliation and lineation stay fixed in an external frame of reference, and after theoretical infinite strain, crystallographic axes should form a maximum normal to foliation if basal ⟨*a*⟩ is dominant, and parallel to lineation if prism ⟨*c*⟩ is dominant. In effect, a body of rock deforming under pure shear *may be divided into domains,* some deforming by incremental left-lateral simple shear and a clockwise back rotation, and some deforming by incrementally right-lateral simple shear and an anticlockwise back rotation (Cobbold & Gapais 1986, Gapais & Cobbold 1987).

It follows that domains deforming right laterally and utilizing either the basal ⟨*a*⟩ system or the prism ⟨*c*⟩ system will behave as described above for dextral simple shear. The conjugate domains deforming by left-lateral

shear and back rotation would form the exact mirror image pattern, thus giving an orthorhombic symmetry to the fabrics.

The *c*-axis fabric for slip on the prism ⟨*a*⟩ system is identical for both pure and simple shear irrespective of the amount of strain. This slip system obviously has a large role to play in the production of the Group C fabrics, and a minor role in others.

The *c*-axis fabrics belonging to Group A can be well explained by dominant prism ⟨*c*⟩ slip under right-lateral simple shear, consistent with the mica fish indicating east-side-down shear. However, the *c*-axis maxima for all of the other groups are not consistently disposed with respect to foliation and lineation, even though mica fish consistently indicate east-side-down shear (Fig. 3). This suggests that the prism ⟨*c*⟩ maximum could have been passively rotated, such that a combination of a single slip system with simple or pure shear cannot fully account for the observed fabrics. We therefore propose to investigate the effect of transitions between slip systems during simple strain histories. In the following sections, we will consider the transitions from prism ⟨*c*⟩ to basal ⟨*a*⟩ slip under simple shear, pure shear and a combination of the two.

The models involve dominant prism ⟨*c*⟩ slip up to some strain (which can be large), followed by a transition to dominant basal ⟨*a*⟩ slip. The transition may be brought about purely by a change in external conditions (lowering temperature, drying rock?); no change in the type of strain is needed.

In *simple shear,* if prism ⟨*c*⟩ slip has operated up to large strain, the *c*-axes are concentrated around the lineation. When the transition to dominant basal ⟨*a*⟩ slip occurs, two populations of grains have to be considered. Grains with their basal ⟨*a*⟩ planes within 45° either way of the shear plane will slip on the basal ⟨*a*⟩ system and rotate so that their basal planes become parallel with the shear plane. This will tend to develop a *c*-axis maximum perpendicular to the shear plane. On the other hand, grains with basal planes oriented at an angle greater than 45° away from the shear plane will slip in a sympathetic manner. With increasing shear, these slip planes must rotate towards the foliation, and they are in such an orientation that slip with an opposite shear sense must occur. Because this orientation is not favorable for slip, the maximum produced thereby is not expected to be as strong as the maximum resulting from easy slip. However, since a pre-existing prism ⟨*c*⟩ maximum is already well developed in this position, this maximum will simply rotate.

This mechanism can account for none of the *c*-axis fabrics seen within the Oakhurst Mylonite Belt, except for that observed in specimen 97 (Group E).

In the *pure shear* transition model, as stated before, the rock body is considered to be domainal on a grain scale. For the first stages of deformation under prism ⟨*c*⟩ slip, the fabric patterns produced would contain two maxima at ±45° to lineation, which would coalesce on the lineation at infinite shear. Considering the case of a transition after infinite pure shear, all the prism planes would be parallel to the foliation and all the basal planes would contain the maximum shortening direction making slip on basal ⟨*a*⟩ difficult. If the prism ⟨*c*⟩/basal ⟨*a*⟩ transition took place at any earlier stage of deformation however, then the grains that were slipping in a right-lateral sense on the prism ⟨*c*⟩ slip are now able to slip in a left-lateral sense on basal ⟨*a*⟩ and vice versa. This is expected to cause the prism ⟨*c*⟩ maximum to rotate away from the lineation. However, after infinite shear with the basal ⟨*a*⟩ system operating, the four maxima would merge into one at the pole to the foliation, with the sole exception of the case where prism ⟨*c*⟩ slip went to infinite strain. Once again this model does not explain the observed fabrics, except perhaps for that of specimen 97.

In the *mixed pure and simple shear model* (Fig. 4), we impose a small amount of simple shear on the system, i.e. deformation has a 'semi-non-coaxial' history. If the simple shear component is right-lateral then, during the first stages of prism ⟨*c*⟩ operation, one maximum would tend to develop at 45° clockwise from lineation and would rotate towards lineation as deformation proceeds. After the transition to basal ⟨*a*⟩ slip, significant differences from the previous models are expected. All grains within the upper-left and lower-right quadrants would be able to slip by right-lateral shear. In the other regions, including those containing any prism ⟨*c*⟩ maximum, there will be a competition between two deformation mechanisms. Firstly, there would be some grains in an orientation favorable for sympathetic slip, as in the simple shear transition model. Secondly, there would be some grains which, during right lateral shear, would show little or no slip in the right-lateral sense, because of their unfavorable orientation. These grains may back-rotate in order to maintain continuity with their neighbors (see fig. 3 in Mainprice & Nicolas 1989). The closer the initial maximum due to ⟨*c*⟩ slip lies to the foliation, the more probable is the latter effect. If this back rotation is significant, then the *c*-axes may rotate past the lineation, where right-lateral slip can now be easily activated. These grains would slip until the maximum lies on the perpendicular to the foliation at theoretically infinite shear. In the former case, the *c*-axes would rotate back to a position on the normal to the foliation after infinite shear, but would never have progressed past the position of the lineation.

One major implication of this scenario is that the prism ⟨*c*⟩ maximum will rotate past the lineation. This rotation is more likely if large strain is accommodated by prism ⟨*c*⟩ slip prior to the basal ⟨*a*⟩ transition (compare second and third paths in Fig. 4). The degree of rotation also depends on the proportion of simple shear, the more simple shear, the less back rotation.

The qualitative models presented above are in effect in two dimensions, and cannot account for maxima other than those at the periphery of the stereonet. Computer models have been used to simulate three-dimensional fabric development during progressive plastic deformation (Lister *et al.* 1978, Lister & Paterson 1979, Lister & Hobbs 1980, Etchecopar & Vasseur 1987). Jessell's

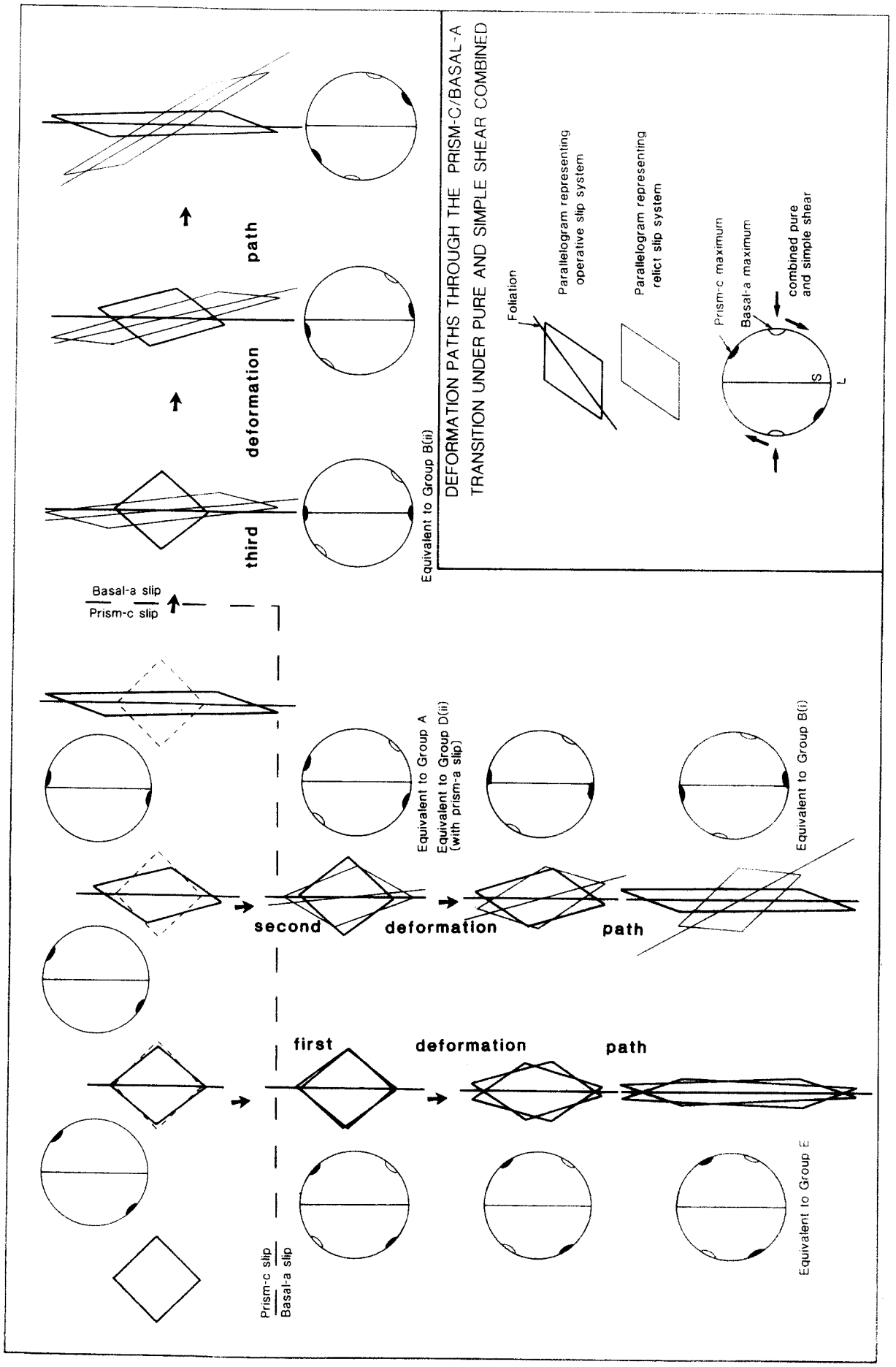


Fig. 4. Schematic illustration of three possible deformation paths through the prism ⟨c⟩-basal ⟨a⟩ transition under a combination of pure shear and dextral simple shear (two-dimensional reference), showing the progressive rearrangement of slip systems and the corresponding expected *c*-axis fabric diagrams (see Fig. 2 for comparison). The finite foliation (S) and lineation (L) are kept fixed, and consequently, the shear plane (not represented here) rotates. The transition from prism ⟨c⟩ slip to basal ⟨a⟩ slip occurs after increasing cumulative prism ⟨c⟩ slip from first to third path. Note that a greater rotation of the prism ⟨c⟩ maximum occurs in the third path, compared to the second path. The rotation past the lineation in the second and third path is made possible owing to the possible back rotation of grains (Mainprice & Nicolas 1989). See text for further discussion.

models (1988b) have demonstrated the importance of recrystallization in the formation, preservation and disappearance of preferred orientation maxima, a mechanism that probably plays an important role in the rocks examined in this paper. All of these studies have attempted to reproduce the more commonly observed basal ⟨a⟩ and prism ⟨a⟩ fabrics, but have generally ignored the effect of prism ⟨c⟩ slip. This type of modeling would allow a more quantitative relationship to be determined between kinematics and petrofabric development in the Oakhurst Mylonite Belt.

*Relationship between grainsize and crystallographic fabric*

Different types of fabrics occur in the same sample within layers of different grainsize. The three largest grainsizes (larger than 0.25 mm, Groups A, B and C, Fig. 2) may be separated from the two smallest (Groups D and E), on a compositional basis, the former being almost pure quartz presumably derived from quartz veins, the latter containing almost all of the mica within each specimen.

According to the kinematic models above, Group A samples (which display the largest grainsize) underwent only minor prism ⟨c⟩ deformation before the transition to basal ⟨a⟩, and then deformation occurred in the basal ⟨a⟩ regime until it ceased. In contrast, rocks in the other groups presumably underwent extensive prism ⟨c⟩ deformation before the transition, since the prism ⟨c⟩ maxima are generally oriented in a position past the lineation (Fig. 4). Therefore, both the grainsize and the fabric can, to some extent, be associated with the duration of exposure to strain, later quartz veins undergoing less prism ⟨c⟩ slip, and preserving a larger grainsize.

Assuming again that our proposed kinematic scenario is correct, Group D shows relatively extensive deformation under prism ⟨c⟩, and then moderate deformation on basal ⟨a⟩ (with, in some cases, slip of prism ⟨a⟩). Group E shows a very intense deformation on basal ⟨a⟩, presumably preceded by deformation on prism ⟨c⟩ (although this is pure conjecture). Thus, the variations of fabric patterns with grainsize can tentatively be correlated with the intensity and timing of slip system transition in the model involving pure shear, with a component of east-side-down simple shear. However, this is only one possible interpretation, and more work on finer microstructures (subgrains, dislocations) should be done to test the correlation between all strain sensitive microstructures and types of slip systems. In addition, it is imperative to study the potentially drastic effect of dynamic recrystallization (Gapais & Barbarin 1986, Jessell 1988b).

## CONCLUSION

Epidote–amphibolite facies quartzites of the Oakhurst Mylonite Belt, California, display unusual quartz *c*-axis fabrics, and are interpreted as resulting from the activation of prism ⟨c⟩ slip. Meso- and microscopic shear criteria suggest that sense of shear in these rocks was rather uniform, consistent with an east-side-down shear movement. Using this constraint, the *c*-axis fabrics are best explained by a model of combined pure and simple shear deformation, during which a transition from prism ⟨c⟩ to basal ⟨a⟩ and prism ⟨a⟩ slip occurs. In this model, the location of *c*-axis maxima depends on when the transition between slip systems takes place relative to the intensity of the first developed, prism ⟨c⟩ slip fabric. For example, supposedly late, coarse grained syntectonic quartz veins record only the latest increments of deformation compared to the quartzite finer grains, resulting in an apparent relationship between grainsize and type of microfabric.

The reasons for the occurrence of prism ⟨c⟩ slip in these rocks are largely unknown. By analogy to the adjacent Bear Mountain fault zone in California, where more detailed metamorphic studies have been carried out, it is proposed that the circulation of hot fluids is at the origin of hydrolytic weakening of quartz, promoting prism ⟨c⟩ slip. The fabric transitions proposed here could then be associated with a combined effect of decreasing temperature under progressively dryer conditions. The role played by the dynamic growth of favorably oriented grains in the production of the observed fabrics is not known, but no particular microstructural feature points to this mechanism being dominant.

*Acknowledgements*—The authors wish to express their gratitude to Jim Stout for useful discussions regarding petrological problems encountered, Scott Paterson, Othmar Tobisch and Richard Schweickert for useful discussions regarding the regional geology of the area, John Platt and an anonymous reviewer for thoughtful comments on the manuscript, Jean-Luc Bouchez for a very constructive and meticulous review, and Rick Thomas and A. Wiggins for assistance in the field. J. M. Garbutt was supported by the University of Minnesota Graduate School, in the form of a University of Minnesota–Cambridge University Exchange Scholarship. A McKnight-Land Grant Professorship awarded to C. Teyssier is gratefully acknowledged.

## REFERENCES

Avé Lallemant, H. G. & Carter, N. L. 1971. Pressure dependence of quartz deformation lamellae orientations. *Am. J. Sci.* **270**, 218–235.

Bateman, P. C., Busacca, A. J. & Sawka, W. N. 1983. Cretaceous deformation in the western Foothills of the Sierra Nevada, California. *Bull. geol. Soc. Am.* **94**, 30–42.

Behr, H. J. 1980. Polyphase shear zones in the granulite belts along the margins of the Bohemian Massif. *J. Struct. Geol.* **2**, 249–254.

Bell, T. H. 1978. Progressive deformation and reorientation of fold axes in a ductile mylonite zone: the Woodroofe Thrust. *Tectonophysics* **44**, 285–320.

Blacic, J. D. 1975. Plastic-deformation mechanisms in quartz: the effect of water. *Tectonophysics* **27**, 271–294.

Blumenfeld, P., Mainprice, D. & Bouchez, J.-L. 1986. *C*-slip in quartz from subsolidus deformed granite. *Tectonophysics* **127**, 97–115.

Bouchez, J.-L., Lister, G. S. & Nicolas, A. 1983. Fabric asymmetry and shear sense in movement zones. *Geol. Rdsch.* **72**, 401–419.

Bouchez, J.-L., Mainprice, D. H., Trepied, L. & Doukhan, J. C. 1984. Secondary lineation in a high-T quartzite (Galicia, Spain): an explanation for an abnormal fabric. *J. Struct. Geol.* **6**, 159–165.

Bouchez, J.-L. & Pecher, A. 1981. The Himalayan Main Central Thrust pile and its quartz rich tectonites in central Nepal. *Tectonophysics* **78**, 23–50.

Cloos, E. 1946. Lineation: a critical review and annotated bibliography. *Mem. geol. Soc. Am.* **18**.

Cobbold, P. R. & Gapais, D. 1987. Slip-system domains. I. Plane-strain kinematics of arrays of coherent bands with twinned fiber orientations. *Tectonophysics* **131**, 113–132.

Culshaw, N. J. & Fyson, W. K. 1983. Quartz ribbons in high grade granite gneiss: modification of dynamically formed quartz c-axis preferred orientation by oriented grain growth. *J. Struct. Geol.* **6**, 663–668.

Duebendorfer, E. M. & Houston, R. S. 1987. Proterozoic accretionary tectonics at the southern margin of the Archean Wyoming craton. *Bull. geol. Soc. Am.* **98**, 554–568.

Duebendorfer, E. M. & Houston, R. S. 1990. Structural analysis of a ductile-brittle Precambrian shear zone in the Sierra Madre, Wyoming: Western extension of the Cheyenne Belt? *Precambrian Res.* **48**, 21–39.

Etchecopar, A. & Vasseur, G. 1987. A 3-D kinematic model of fabric development in polycrystalline aggregates: comparisons with experimental and natural examples. *J. Struct. Geol.* **9**, 705–717.

Gapais, D. & Barbarin, B. 1986. Quartz fabric transition in a cooling syntectonic granite (Hermitage Massif, France). *Tectonophysics* **125**, 357–370.

Gapais, D. & Cobbold, P. R. 1987. Slip-system domains. 2. Kinematic aspects of fabric development in polycrystalline aggregates. *Tectonophysics* **138**, 289–309.

Garbutt, J. M. 1989. A kinematic analysis of the Oakhurst Mylonite Belt, Sierra Nevada Foothills, California. Unpublished Masters thesis, University of Minnesota.

Geffel, M. J., Twiss, R. J. & Moores, E. M. 1989. Ductile and brittle shear sense for the Melones Fault Zone, northern Sierra Nevada, California. *Geol. Soc. Am. Abs. w. Prog.* **21**, 83.

Giletti, B. J. & Yund, R. A. 1984. Oxygen diffusion in quartz. *J. geophys. Res.* **89**, 4039–4046.

Griggs, D. T. & Blacic, J. D. 1965. Quartz: anomalous weakness of synthetic crystals. *Science* **147**, 292–295.

Hobbs, B. E. 1985. The geological significance of microfabric analysis. In: *Preferred Orientation in Deformed Metals and Rocks: An Introduction to Modern Texture Analysis* (edited by Wenk, H.-R.). Academic Press, London, 463–484.

Hobbs, B. E., McLaren, A. C. & Paterson, M. S. 1972. Plasticity of single crystals of synthetic quartz. In: *Flow and Fracture of Rocks* (edited by Heard, H. C., Borg, I. Y., Carter, N. L. & Raleigh, C. B.). *Am. Geophys. Un. Geophys. Monogr.* **16**, 29–53.

Jessell, M. W. 1988a. Simulation of fabric development in recrystallizing aggregates—I. Description of the model. *J. Struct. Geol.* **10**, 771–778.

Jessell, M. W. 1988b. Simulation of fabric development in recrystallizing aggregates—II. Example model runs. *J. Struct. Geol.* **10**, 779–793.

Law, R. D. 1986. Relationships between strain and quartz crystallographic fabrics in the Roche Maurice quartzites of Plougastel, western Brittany. *J. Struct. Geol.* **8**, 493–515.

Law, R. D., Casey, M. & Knipe, R. J. 1986. Kinematic and tectonic significance of microstructures and crystallographic fabrics within quartz mylonites from the Assynt and Eriboll regions of the Moine Thrust zone, NW Scotland. *Trans. R. Soc. Edinb. Earth Sci.* **77**, 99–125.

Linker, M. F. & Kirby, S. H. 1981. Anisotropy in the rheology of hydrolytically weakened synthetic quartz crystals. In: *Mechanical Behavior of Crustal Rocks. Am. Geophys. Un. Geophys. Monogr.* **24**, 29–60.

Lister, G. S. & Dornsiepen, U. F. 1982. Fabric transitions in the Saxony granulite terrain. *J. Struct. Geol.* **4**, 81–92.

Lister, G. S. & Hobbs, B. E. 1980. The simulation of fabric development during plastic deformation and its application to quartzites: the influence of deformation history. *J. Struct. Geol.* **2**, 355–370.

Lister, G. S. & Paterson, M. S. 1979. The simulation of fabric development during plastic deformation and its application to quartzites: fabric transitions. *J. Struct. Geol.* **1**, 99–115.

Lister, G. S., Paterson, M. S. & Hobbs, B. E. 1978. The simulation of fabric development in plastic deformation and its application to quartzites: the model. *Tectonophysics* **45**, 107–158.

Lister, G. S. & Price, G. P. 1978. Fabric development in a quartz feldspar mylonite. *Tectonophysics* **49**, 37–78.

Lister, G. S. & Snoke, A. W. 1984. S–C mylonites. *J. Struct. Geol.* **6**, 617–638.

Lister, G. S. & Williams, P. F. 1979. Fabric development in shear zones: theoretical controls and observed phenomena. *J. Struct. Geol.* **1**, 283–297.

Lister, G. S. & Williams, P. F. 1983. The partitioning of deformation in flowing rock masses. *Tectonophysics* **92**, 1–33.

Mainprice, D. & Nicolas, A. 1989. Development of shape and lattice preferred orientations: application to the seismic anisotropy of the lower crust. *J. Struct. Geol.* **11**, 175–189.

Nicolas, A. & Poirier, J. P. 1976. *Crystalline Plasticity and Solid State Flow in Metamorphic Rocks*. Wiley, London.

Paterson, S. R., Tobisch, O. T. & Bhattacharyya, T. 1989. Regional, structural and strain analyses of terranes in the Western Metamorphic Belt, central Sierra Nevada, California. *J. Struct. Geol.* **11**, 255–273.

Paterson, S. R., Tobisch, O. T. & Radloff, J. K. 1987. Post-Nevadan deformation along the Bear Mountains Fault Zone: Implications for the Foothills terrane, central Sierra Nevada, California. *Geology* **15**, 513–516.

Price, G. P. 1985. Preferred Orientations in quartzites. In: *Preferred Orientations in Deformed Metals and Rocks: An Introduction to Modern Texture Analysis* (edited by Wenk, H.-R.). Academic Press, London, 385–406.

Schmid, S. M. & Casey, M. 1986. Complete fabric analysis of some commonly observed quartz c-axis patterns. In: *Mineral and Rock Deformation: Laboratory Studies—The Paterson Volume* (edited by Hobbs, B. E. & Heard, M. C.). *Am. Geophys. Un. Geophys. Monogr.* **36**, 263–286.

Schmid, S. M., Casey, M. & Starkey, J. 1981. An illustration of the advantages of a complete texture analysis described by the orientation distribution function (ODF) using quartz pole figure data. *Tectonophysics* **78**, 101–117.

Simpson, C. 1986. Determination of movement sense in mylonites. *J. Geol. Educ.* **34**, 246–261.

Simpson, C. & Schmid, S. M. 1983. An evaluation of criteria to deduce the sense of movement in sheared rocks. *Bull. geol. Soc. Am.* **94**, 1281–1288.

Tobisch, O. T., Paterson, S. R., Saleeby, J. B. & Geary, E. E. 1989. Nature and timing of deformation in the Foothills terrane, central Sierra Nevada, California: Its bearing on orogenesis. *Bull. geol. Soc. Am.* **101**, 401–413.

Tullis, J. A. & Tullis, T. E. 1972. Preferred orientation produced by mechanical Dauphine twinning: Thermodynamics and axial experiments. *Am. Geophys. Un. Geophys. Monogr.* **16**, 67–82.

Vissers, R. L. M. 1989. Asymmetric c-axis fabrics and flow vorticity: a study using rotated garnets. *J. Struct. Geol.* **11**, 231–244.